The Journal of Phytopharmacology 2024; 13(5):374-382
Online at: www.phytopharmajournal.com

Research Article

ISSN 2320-480X
JPHYTO 2024; 13(5): 374-382
September- October
Received: 11-08-2024
Accepted: 22-10-2024

doi: 10.31254/phyto.2024.13506

Anoopa Satheesan
Department of Veterinary Pharmacology and Toxicology, College of Veterinary and Animal Sciences, Mannuthy-680651, Thrissur, Kerala, India

Siyana Saleem P
Department of Veterinary Pharmacology and Toxicology, College of Veterinary and Animal Sciences, Mannuthy-680651, Thrissur, Kerala, India

Suresh N Nair
Department of Veterinary Pharmacology and Toxicology, College of Veterinary and Animal Sciences, Mannuthy-680651, Thrissur, Kerala, India

Bibu John Kariyil
Department of Veterinary Pharmacology and Toxicology, College of Veterinary and Animal Sciences, Mannuthy-680651, Thrissur, Kerala, India

Nisha AR
Department of Veterinary Pharmacology and Toxicology, College of Veterinary and Animal Sciences, Mannuthy-680651, Thrissur, Kerala, India

Deepthi Vijay
Department of Veterinary Public Health, College of Veterinary and Animal Sciences, Mannuthy- 680651, Thrissur, Kerala, India

Prasanna KS
Department of Veterinary Pathology, College of Veterinary and Animal Sciences, Mannuthy- 680651, Thrissur, Kerala, India

Correspondence:
Dr. Suresh N. Nair
Department of Veterinary Pharmacology and Toxicology, College of Veterinary and Animal Sciences, Mannuthy-680651, Thrissur, Kerala, India
Email: suresh@kvasu.ac.in

In silico assessment of wound healing activity of phytochemicals from methanolic extract of *Plectranthus amboinicus* (Lour.) Spreng

Anoopa Satheesan, Siyana Saleem P, Suresh N Nair, Bibu John Kariyil, Nisha AR, Deepthi Vijay, Prasanna KS

ABSTRACT

Background: Evaluating the wound healing potential of ligands present in a crude extract through molecular docking studies targeting TNF-α, IL-1β, and TGF-β1 is highly informative. TNF-α and IL-1β are key pro-inflammatory cytokines involved in the inflammatory phase of wound healing, whereas TGF-β1 plays a crucial role in tissue regeneration and remodelling. By assessing the binding affinity and interactions of the extract's phytochemicals with these proteins, valuable insights into the extract's potential anti-inflammatory and regenerative effects can be gained. This approach facilitates a targeted evaluation of the extract's capacity to modulate critical pathways in wound healing, thereby providing essential information for developing effective therapeutic agents. Aims and Objectives: Molecular docking studies on phytochemicals derived from the methanolic extract of *Plectranthus amboinicus* targeting TNF-α, IL-1β, and TGF-β1 provide insights into the potential wound healing efficacy of the *Plectranthus amboinicus* leaf extract, as reflected by the obtained docking scores. Materials and Methods: Chemical profiling of the methanolic leaf extract of *Plectranthus amboinicus* was conducted using GC-MS. In silico molecular docking studies with AutoDock4 were employed to evaluate the binding of these phytoconstituents to the active sites of three proteins associated with wound healing: TNF-α, TGF-β1, and IL-1β. Additionally, the pharmacokinetic properties of the active compounds were further assessed using the admetSAR software. Results and Conclusion: Of the compounds identified by GC-MS analysis, 13 exhibited promising binding scores, indicating a hopeful wound healing potential for the plant. AdmetSAR predictions further suggested that these phytoconstituents possess favourable absorption, distribution, and metabolism profiles, with low toxicity. Collectively, these findings suggest that the methanolic leaf extract of *Plectranthus amboinicus* holds significant wound healing activity.

Keywords: GCMS, AutoDock4, admetSAR, TNF-α, IL-β1, TGF-β1.

INTRODUCTION

The wound healing process comprises four closely interconnected and overlapping phases: Haemostasis, inflammation, proliferation, and tissue remodelling. These phases and their respective biophysiological functions necessitate precise sequential occurrence, specific timing, and optimal intensity throughout a specified duration. Numerous factors can potentially influence wound healing, consequently interfering with one or more phases of the process, thus resulting in inadequate or impaired tissue repair [1].

In chronic wounds, persistent inflammation leads to high levels of pro-inflammatory cytokines such as interleukin-1β (IL-1β) and tumour necrosis factor α (TNFα), which cause excessive protease activity and destruction of the extracellular matrix (ECM). Additionally, chronic wounds are characterized by the release of specific factors like transforming growth factor-beta (TGF-β). These factors contribute to the disordered repair process in chronic wounds [2]. The appropriate expression of pro-inflammatory cytokines (IL-1β and TNF-α) is essential for recruiting neutrophils to the wound site. These cytokines also stimulate the production of metalloproteinases (MMP) in inflammatory and fibroblast cells. MMP aids in the removal of damaged extracellular matrices (ECM) during wound healing to facilitate repair [3].

Plectranthus amboinicus (Lour.) Spreng, a perennial herb classified within the Lamiaceae family, is renowned for its therapeutic and nutritional attributes, which can be attributed to its rich repository of natural phytochemical compounds [4]. The herb has a long history of traditional use and has been known for its effectiveness in folkloric medicines for many years. It is particularly impressive in its ability to promote wound healing with minimal side effects. Laboratory tests on mice have shown that *P. amboinicus*, has no noticeable adverse effects, making it truly remarkable in this aspect [5].

Molecular docking is a method that uses computer simulations to predict how molecules interact at the atomic level. This technique can be used to understand how plant-based compounds interact with specific molecular targets associated with wound healing. By virtually fitting these compounds into the target structures, we can learn about their binding strength, affinity and modes of interaction. This approach is extremely valuable for designing new drugs and identifying potential treatments [6].

ADMET properties, encompassing absorption, distribution, metabolism, excretion, and toxicity, are crucial for evaluating safety and risk. Although typically examined through *in vivo* and *in vitro* studies, these approaches can be costly and time-consuming. *In silico* methods, such as the admetSAR platform, have been developed as faster and more economical alternatives, leveraging machine learning-driven QSAR models to predict these properties before compound synthesis [7].

This study will contribute to the advancement of innovative and efficient therapies that can supplement or potentially substitute traditional treatments for wound healing, providing fresh optimism for patients dealing with difficult wound healing situations. The utilization of plant extracts can also help avoid the issues linked to the side effects of standard medical treatments.

MATERIAL AND METHODS

Preparation of methanolic extract of leaves of *Plectranthus amboinicus*

The leaves of *Plectranthus amboinicus* were dried at room temperature and coarsely powdered using an electric pulveriser. The powder obtained was extracted using a Soxhlet apparatus with methanol. The methanol extract was then concentrated using a rotary vacuum evaporator under reduced pressure and temperature [8].

Identification of potential ligands from the extract

The GC-MS analysis of the crude extract of *P. amboinicus* was conducted at the Centre for Analytical Instrumentation- Kerala (CAI-K) of the Kerala Forest Research Institute (KFRI) in Peechi, Kerala. The analysis was performed using a Gas Chromatography Mass Spectrometer (Shimadzu Nexus GC- 2030) with a mass range of 1.5-1000 m/z. Helium was utilized as the carrier gas at a flow rate of 1 mL/min. The oven temperature was initially set at 60° C and then raised to 280° C within 5 minutes. The injector temperature was maintained at 260 °C, and the total analysis time was 50 minutes. After obtaining a clear baseline, aliquots of the extracts (0.4 µL) were injected into the chromatographic column. The major constituents were identified using NIST 20 mass spectrum library [9].

Preparation of receptor and ligand

The ligand structures were obtained from the PubChem Compound Database (National Center for Biotechnology Information; https://pubchem.ncbi.nlm.nih.gov/) in Spatial Data File (.SDF) format. These structures were then processed with Marvin View 17.25.0 (www.chemaxon.com) and converted to the Tripos Mol2 format. Using the modifying tools of ADT, ligands were processed by detecting roots, expanding roots, and selecting the number of rotatable bonds. After these initial preparations, the ligand molecules were converted to PDBQT format for use in AutoDock4.

Receptor structures for interleukin-β1 (IL-β1) (AlphaFold ID: Q63264 for rat), tumor necrosis factor-α (TNFα) (AlphaFold ID: P16599 for rat), and transforming growth factor beta receptor 1 (TGF-β1) (AlphaFold ID: P17246 for rat) were downloaded from AlphaFold Protein Structure Database in PDB format [10]. The structures were prepared for further processing and docking using Accelrys Discovery Studio Visualizer 3.5.0.12158 (Copyright© 2005-12, Accelrys Software Inc). Subsequently, the macromolecules were processed in AutoDock 1.5.6 (Molecular Graphics Laboratory tools, www.mgltools.scripps.edu) following the standard protocol and parameters outlined in the AutoDock Tools (ADT) tutorial [6].

Docking methodology

Docking studies were performed using AutoDock4, developed by the Scripps Research Institute (La Jolla, CA, www.autodock.scripps.edu). The grid map for this study was calculated with AutoDock4. The Computed Atlas of Surface Topography of Proteins (CASTp) server (http://cast.engr.uic.edu) was used to pinpoint the active sites in the proteins. By submitting the target protein to the CASTp server, it forecasts the key amino acids involved in binding interactions, facilitating the prediction of ligand binding sites and aiding in docking studies [11]. The grid centre was set as follows. For TNFα the X, Y and Z coordinates were -38.8902, 9.75843 and 7.47827 respectively. For IL-β1 the X, Y and Z coordinates were -13.2108, 27.28682 and -22.1551 respectively. For TGF-β1 the X, Y and Z coordinates were -4.376138, 1.540179 and 5.792581 respectively. The processed file was saved in grid parameter file (gpf) format. Using parameters optimized by ADT, the docking parameter file (dpf) was created. The Lamarckian genetic algorithm was employed for all docking runs. The docking log (dlg) file, which included an RMSD table, provided the binding energy (KCal/mol) for each molecule's optimal docked configurations.

Visualisation of results

Post-docking analysis, including the identification of binding site locations, hydrogen-bond interactions, hydrophobic interactions, and bonding distances, was conducted using LigPlot and Discovery Studio Visualizer. The optimal and most energetically favourable conformations of each ligand were selected by examining their binding poses and characterizing their interactions with the protein [6].

Assessment of *in silico* pharmacokinetics of the phytochemicals

Ligands were obtained from PubChem in SMILES format [12]. These SMILES representations of the selected ligands were then submitted to the AdmetSAR online tool (http://lmmd.ecust.edu.cn/admetsar2/) to evaluate their toxicity [13]. The pharmacokinetic properties and the possible toxicities were interpreted as per the standard protocol.

RESULTS

Figure 1. shows the GC-MS chromatogram obtained for the plant extract. The phytochemicals obtained on GC-MS analysis are listed in Table 1. Ligands were docked against different proteins of wound healing such as TNF-α, IL-β1 and TGF-β1. The binding energies of different ligands obtained from the RMSD table and the list of hydrogen bonds and hydrophobic interactions of the potential ligands are consolidated in Table 2. Figure 2 shows the post-docking analysis of docked pose and ligplot interactions of the ligand with receptors (hydrogen bonds and hydrophobic interactions).

Among 28 different compounds, 13 compounds exhibited moderately higher binding energies against all three receptors. Seven phytochemicals formed hydrogen bonds with TNF-α, eight with IL-β1 and nine with TGF-β1. The ligands with better docking scores against TNF-α, IL-β1 and TGF-β1 are shown in Table 2.

In silico analysis of pharmacokinetics and toxicity profile of selected ligands are listed in Table 3 and Table 4. The study results indicate that most compounds pose a greater risk of central nervous system (CNS) effects at toxic doses. There is an increased likelihood of toxicity at lower doses due to enhanced intestinal absorption. Specifically, compounds such as 2-methyl-5-(1-methylethyl)-phenol, p-Cymene-2,5-diol, 1H-Cycloprop[e]azulen-7-ol, and (Z,Z,Z)-9,12,15-Octadecatrienoic acid methyl ester may inhibit the bioavailability of other chemicals. This inhibition can amplify toxicity by increasing the activity of P-glycoprotein. Additionally, some

compounds may disrupt sodium, potassium, and calcium homeostasis by affecting renal organic cation transporters. Several compounds also influence the metabolism of other chemicals by acting as substrates for CYP450 2C9 and inhibitors of CYP 450 3A4 and CYP 450 2D6.

Toxicity assessments revealed that most compounds are mutagenic at higher doses, and some are potential carcinogens. Furthermore, these compounds are ecotoxic, particularly to fish, and may pose risks to arthropods and protozoa. The potential for residual effects is minimal, as the probability of biodegradation is low.

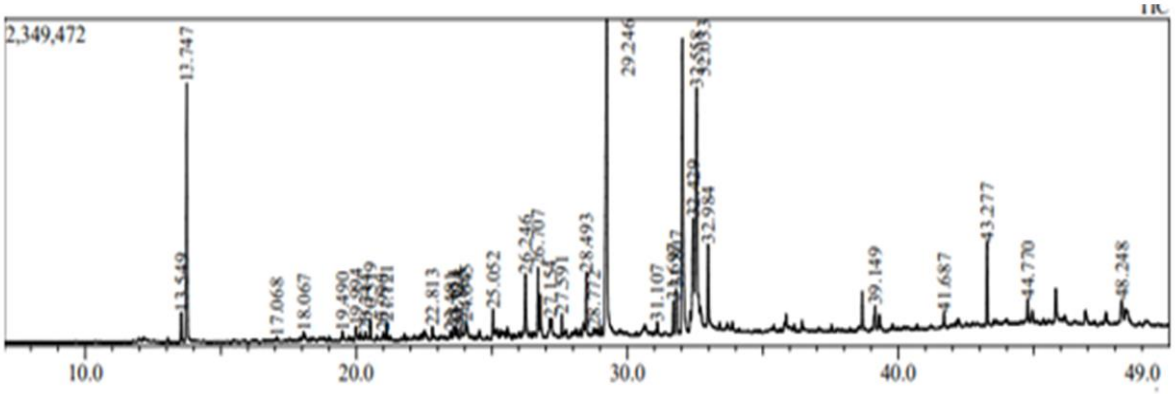

Figure 1: GC-MS chromatogram of methanolic leaf extract of Plectranthus amboinicus

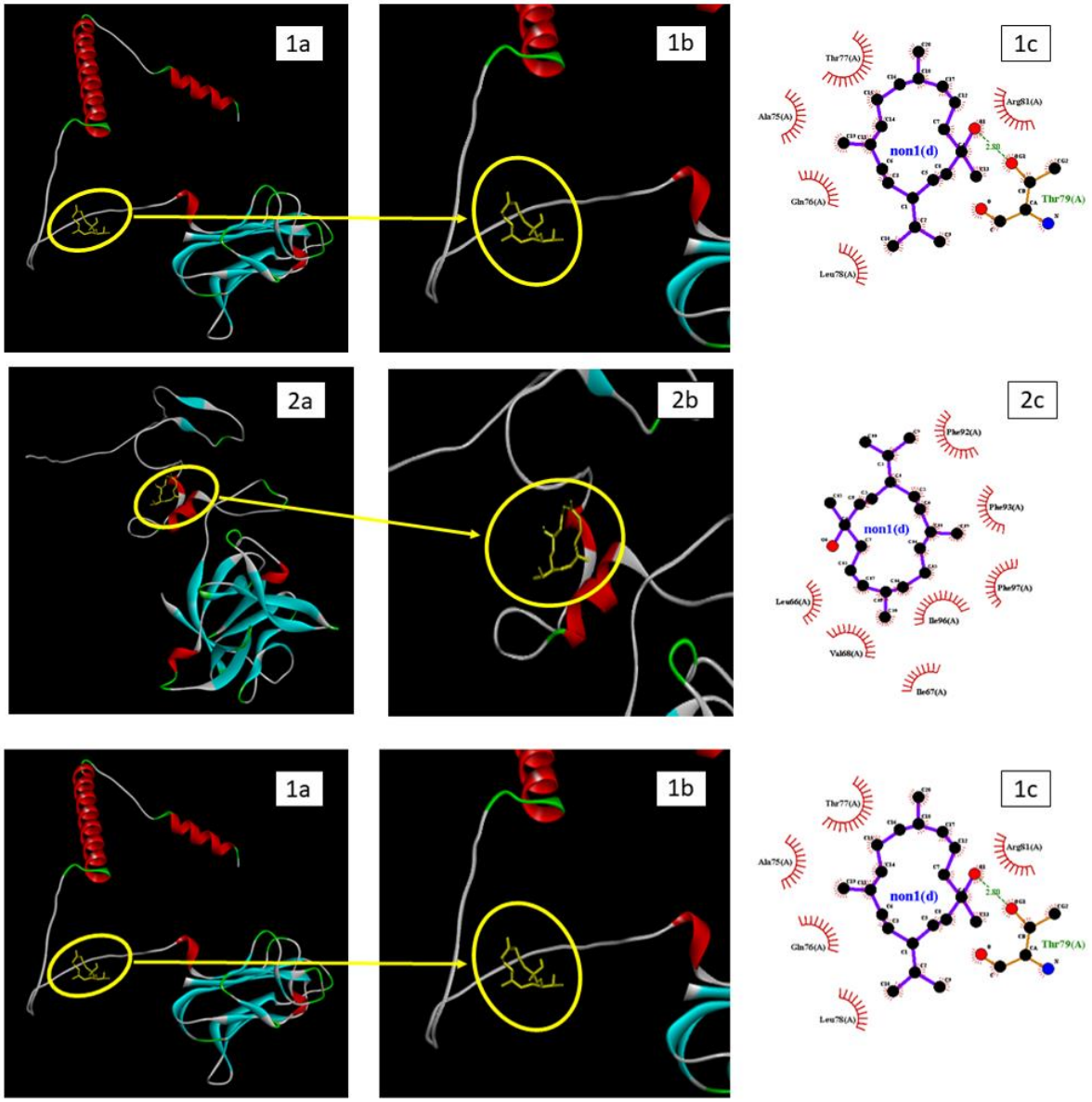

Figure 2: Figure 2: Post-docking interactions of thunbergol against TNF-a, IL-ß1 and (1R,7S,E)-7- Isopropyl-4,10-dimethylenecyclodec-5-enol against TGF-β1. 1a and 1c: In situ docked thunbergol against TNF-a and LigPlot showing their interactions in the docked pose. 2a and 2c: In situ docked thunbergol against IL-B1 and LigPlot showing their interactions in the docked pose. 3a and 3c: In situ docked (1R,7S,E)-7-Isopropyl-4,10-dimethylenecyclodec-5-enol against TGF-β1 and LigPlot showing their interactions in the docked pose. 1b, 2b and 3b: Magnified view illustrating the ligand binding pocket within the receptor molecule

Table 1: List of compounds identified by chemical profiling of the methanolic leaf extract of *Plectranthus amboinicus*

S. No.	LIGAND
1	trans-Ascaridol glycol
2	2-methyl-5-(1-methylethyl)-Phenol
3	Caryophyllene
4	3,4-dimethyl-1-Nonen-4-ol
5	p-Cymene-2,5-diol
6	Dodecanoic acid
7	1H-Cycloprop[e]azulen-7-ol
8	alpha-Cadinol
9	(1R,7S,E)-7-Isopropyl-4,10-dimethylenecyclodec-5-enol
10	Z-8-Octadecen-1-ol acetate
11	1-Ethynylcyclododecanol
12	Thunbergol
13	beta.-Neoclovene
14	Tetradecanoic acid
15	Neophytadiene
16	Pentadecanoic acid
17	Hexadecanoic acid, methyl ester
18	Palmitoleic acid
19	Heptadecanoic acid
20	(Z,Z)-9,12-Octadecadienoic acid, methyl ester
21	(Z,Z,Z)-9,12,15-Octadecatrienoic acid, methyl ester
22	Phytol
23	(Z,Z)-9,12-Octadecadienoic acid
24	Octadecanoic acid
25	Heptacosanal
26	Dotriacontane
27	Squalene
28	(E,E,E,E,E,E)-(1)-2,6,10,15,19,23-Hexamethyltetracosa-1,6,10,14,18,22-hexaen-3-ol

Table 2: Binding energies (KJ/mol) of different ligands obtained from RMSD table and the list of hydrogen bonds and hydrophobic interactions of the potential ligands with TNF-α, IL-β1, TGF-β1

S. No.	LIGAND	TNF-α			IL-β1			TGF-β1		
		Binding energy (KJ/ mol)	No. of Hydrogen bond	Amino acids in hydrophobic interaction	Binding energy (KJ/ mol)	No. of Hydrogen bond	Amino acids in hydrophobic interaction	Binding energy (KJ/ mol)	No. of Hydrogen bond	Amino acids in hydrophobic interaction
1	trans-Ascaridol glycol	-3.54	0	Ala75, Thr77, Thr79, Leu78, Gln76	-4.92	1	Ile47, Val68, Ser65, Leu66, Gln48, Ser46, Ile67	-4.66	0	Asp433, Ser432, Pro434, Lys333, Tyr376, Lys335, Ser334, Thr373, Leu424, Arg375
2	2-methyl-5-(1-methylethyl)-Phenol	-3.51	1	Gln76, Thr77, Leu78, Thr79	-4.75	2	Ile47, Val68, Leu49, Leu66, Ile67, Gln48, Ser46	-4.08	2	Asp433, Lys335, Phe287, Leu424, Tyr376, Lys333, Pro434, Ser432, Arg375
3	Caryophyllene	-3.99	0	Arg81, Thr77, Leu78, Thr79	-4.79	0	Phe92, Phe93, Leu66, Val68, Ile96, Phe97	-5.1	0	Ser432, Thr373, Leu424, Arg375, Pro434, Asp433, Lys335, Phe287, Tyr376, Lys333
4	p-Cymene-2,5-diol	-3.47	0	Thr77, Leu78, Gln76, Leu80	-4.23	1	Leu66, Gln48, Ile47, Ser46, Ile67, Ser65	-4.23	2	Pro434, Asp433, Thr373, Lys335, Lys333, Tyr376, Leu424, Arg375, Ser432
5	1H-Cycloprop[e]azulen-7-ol	-4.41	1	Gln76, Thr77, Leu78, Arg81, Thr79	-5.54	2	Ser46, Ile47, Phe97, Leu66, Val68, Ala69, Ile67	-5.23	1	Phe287, Lys333, Asp433, Pro434, Arg375, Ser432, Thr373, Tyr376, Leu424, Lys335
6	alpha-Cadinol	-4.43	2	Thr77, Leu78, Gln76, Thr79, Arg81	-5.49	1	Phe97, Gln48, Ile47, Leu66, Ile67, Ala69, Val68, Ser46	-5.13	1	Pro434, Asp433, Lys333, Thr373, Tyr376, Ser334, Lys335, Leu424, Arg375, Ser432
7	(1R,7S,E)-7-Isopropyl-4,10-dimethylenecyclodec-5-enol	-4.26	1	Gln76, Ala75, Arg81, Leu78, Thr77, Thr79	-5.25	1	Phe92, Ile96, Phe93, Phe97, Leu66, Ile67, Val68	-5.28	2	Pro434, Lys335, Lys333, Thr373, Tyr376, Leu424, Arg375, Ser432
8	1-Ethynylcyclododecanol	-4.11	2	Leu78, Arg81, Thr79, Thr77	-5.43	2	Gln48, Phe97, Leu66, Ile47, Ser46, Val68, Ala69, Ile67	-4.69	1	Tyr376, Leu424, Thr373, Arg375, Ser432, Pro434, Asp433, Lys333, Lys335
9	Thunbergol	-4.64	1	Thr77, Gln76, Ala75, Leu78, Thr79, Arg81	-5.9	0	Phe92, Phe93, Phe97, Ile96, Ile67, Val68, Leu66	-5.03	2	Thr373, Tyr376, Lys333, Ser334, Lys335, Pro434, Leu424, Arg375, Ser432
10	beta-Neoclovene	-4.12	0	Thr77, Gln76, Thr79, Leu78	-5.09	0	Phe92, Ile96, Phe97, Leu66, Val68, Phe93	-4.7	0	Lys335, Thr373, Tyr376, Pro434, Arg375, Leu424, Asp433, Ser432
11	(Z,Z,Z)-9,12,15-Octadecatrienoic acid, methyl ester	-2.65	0	Ser72, Ala75, Leu80, Leu78, Thr79, Thr77, Thr77, Gln76, Met74, Ser73	-4.45	0	Val64, Ser65, Leu49, Gln50, Gln48, Ile67, Ser46, Ile47, Leu66	-3.97	1	Tyr427, Gln423, Phe287, Pro434, Thr373, Asp433, Lys335, Ser432, Leu424, Arg375
12	Squalene	-3.13	0	Gln76, Leu78, Thr77, Ser73, Ala75, Arg81, Thr79	-4.03	0	Val70, Ile67, Leu66, Ile96, Phe92, Phe93, Phe97, Val68, Ala69	-3.05	0	Asp288, Ser285, Lys335, Lys211, Arg213, Lys333, Gly212, Ile209
13	(E,E,E,E,E,E)-(1)-2,6,10,15,19,23-Hexamethyltetracosa-1,6,10,14,18,22-hexaen-3-ol	-3.15	1	Leu78, Ala75, Gln76, Thr77, Ser82, Leu80, Thr79, Arg81	-4.5	1	Pro89, Ile96, Phe92, Phe93, Phe97, Val68, Ile67, Leu66, Ser65, Val64	-3.34	1	Lys211, Asn336, Lys333, Ser432, Asp433, Leu424, Asp288, Phe287, Lys335

Table 3: *In silico* pharmacokinetic and toxicity profiles of the selected compounds using admetSAR

LIGANDS / **MODELS**	trans-Ascaridol glycol	2-methyl-5-(1-methylethyl)-Phenol	Caryophyllene	p-Cymene-2,5-diol	1H-Cycloprop[e]azulen-7-ol	alpha-Cadinol	(1R,7S,E)-7-Isopropyl-4,10-dimethylenecyclodec-5-enol	1-Ethynylcyclododecanol	Thunbergol	beta-Neoclovene	(Z,Z,Z)-9,12,15-Octadecatrienoic acid, methyl ester	Squalene	2,6,10,15,19,23-Hexamethyltetracosa-1,6,10,14,18,22-hexaen-3-ol
ABSORPTION													
Blood-Brain Barrier	0.9842	0.9381	0.9536	0.7219	0.9679	0.9455	0.8545	0.9801	0.94	0.9726	0.978	0.9442	0.9133
Human Intestinal Absorption	0.9951	0.9955	0.9926	0.9954	0.9899	1	0.9925	0.9947	1	0.9974	0.9904	0.9895	0.9842
Caco-2 Permeability	0.7173	0.9153	0.6327	0.9222	0.7034	0.8129	0.761	0.7502	0.754	0.6691	0.7822	0.6999	0.7448
P-glycoprotein Substrate	0.5287	0.722	0.5779	0.6797	0.7146	0.7393	0.5656	0.5558	0.618	0.5849	0.6904	0.6068	0.5283
P-glycoprotein Inhibitor	0.642	0.9343	0.5989	0.945	0.9772	0.607	0.667	0.8748	0.7329	0.6875	0.8669	0.723	0.653
P-glycoprotein Non-Inhibitor	0.8648	0.9883	0.6689	0.98	0.9863	0.7894	0.9525	0.8597	0.8879	0.8003	0.7569	0.596	0.6736
Renal Organic Cation Transporter	0.8458	0.9036	0.8269	0.9137	0.8758	0.79	0.8295	0.8637	0.889	0.7044	0.8832	0.8449	0.888
DISTRIBUTION													
Subcellular localization	0.3445	0.8502	0.6916	0.9105	0.4329	0.4594	0.5378	0.5054	0.4231	0.7057	0.5877	0.6684	0.3296
METABOLISM													
CYP450 2C9 Substrate	0.8209	0.7352	0.9004	0.7672	0.7411	0.7872	0.8593	0.7996	0.8567	0.8549	0.8437	0.8412	0.8713
CYP450 2D6 Substrate	0.7789	0.7838	0.8386	0.6043	0.8421	0.8762	0.8535	0.8545	0.8483	0.8538	0.8946	0.8065	0.8381
CYP450 3A4 Substrate	0.633	0.5667	0.5777	0.5673	0.644	0.7468	0.6103	0.506	0.6463	0.6352	0.6235	0.5543	0.5
CYP450 1A2 Inhibitor	0.5742	0.9107	0.6695	0.7668	0.7496	0.8334	0.7513	0.6204	0.7819	0.8204	0.5574	0.7354	0.6713
CYP450 2C9 Inhibitor	0.7987	0.907	0.6249	0.7997	0.7166	0.7	0.8743	0.8031	0.8021	0.6901	0.9432	0.9099	0.8822
CYP450 2D6 Inhibitor	0.9202	0.9368	0.9284	0.9263	0.8031	0.9371	0.9189	0.9412	0.9424	0.9255	0.9519	0.9491	0.9451
CYP450 2C19 Inhibitor	0.6148	0.9026	0.5957	0.8683	0.6859	0.6108	0.8101	0.8244	0.8452	0.547	0.9521	0.9168	0.8807
CYP450 3A4 Inhibitor	0.8628	0.9196	0.8665	0.8694	0.9357	0.8359	0.8963	0.9186	0.8491	0.8252	0.9738	0.9716	0.8624
CYP Inhibitory Promiscuity	0.859	0.7429	0.8433	0.5874	0.8169	0.8326	0.8491	0.8981	0.917	0.5776	0.8346	0.6923	0.8452
TOXICITY													

AMES Toxicity	0.8239	0.9282	0.9167	0.9576	0.7404	0.9157	0.925	0.9428	0.8973	0.8854	0.8828	0.9518	0.9427
Carcinogens	0.7534	0.7195	0.6863	0.7171	0.8667	0.9094	0.8881	0.824	0.8409	0.8012	0.5067	0.5631	0.5738
Fish Toxicity	0.8564	0.8752	0.9858	0.7348	0.7934	0.9598	0.9773	0.5911	0.8421	0.999	0.925	0.9811	0.9757
Tetrahymena Pyriformis Toxicity	0.8896	0.9346	0.9574	0.9236	0.8847	0.9524	0.5098	0.6488	0.7986	0.9898	0.9906	0.9987	0.9789
Honey Bee Toxicity	0.7594	0.8337	0.8459	0.7976	0.8487	0.8609	0.8417	0.788	0.8642	0.8405	0.8144	0.8428	0.8276
Biodegradation	0.8399	0.7808	0.5734	0.7909	0.516	0.9531	0.8301	0.9724	0.8682	0.9517	0.7277	0.7909	0.8671
Acute Oral Toxicity	0.7463	0.8351	0.82	0.8441	0.6007	0.8519	0.7092	0.8162	0.7956	0.808	0.7281	0.8971	0.8538
Carcinogenicity (Three-class)	0.555	0.7172	0.4768	0.7202	0.4425	0.5844	0.6667	0.6488	0.5904	0.4615	0.7586	0.4712	0.6926

Table 4: *In silico* ecotoxicity profile of the ligands predicted using admetSAR

Model	Rat Acute Toxicity	Fish Toxicity	Tetrahymena Pyriformis Toxicity
Unit	LD50, mol/kg	pLC50, mg/L	pIGC50, ug/L
trans-Ascaridol glycol	2.8934	2.003	0.5701
2-methyl-5-(1-methylethyl)-Phenol	2.2996	0.3274	1.065
Caryophyllene	1.4345	-0.4316	0.7432
p-Cymene-2,5-diol	1.8821	0.8441	1.8521
1H-Cycloprop[e]azulen-7-ol	2.6068	0.9799	0.5561
alpha-Cadinol	2.2009	0.5113	0.9825
(1R,7S,E)-7-Isopropyl-4,10-dimethylenecyclodec-5-enol	2.1191	0.8259	0.2355
1-Ethynylcyclododecanol	2.0988	1.0357	0.269
Thunbergol	1.5914	-1.1033	1.3347
beta-Neoclovene	1.6333	0.7919	0.895
(Z,Z,Z)-9,12,15-Octadecatrienoic acid, methyl ester	1.5057	-0.6657	0.9942
Squalene	1.8189	0.1123	0.8523
2,6,10,15,19,23-Hexamethyltetracosa-1,6,10,14,18,22-hexaen-3-ol	1.7397	1.5345	-0.0164

DISCUSSION

GC-MS analysis of the essential oil extracted from fresh *Plectranthus amboinicus* leaves identified 11 compounds of which the major components include carvacrol, thymol, cis-caryophyllene, trans-caryophyllene and p-cymene [14]. Another study found that the methanolic extract of leaves of *Plectranthus amboinicus* had the highest concentrations of total phenolics (94.37 ± 1.24 mg GAE/g) and flavonoids (26.90 ± 1.35 mg RE/g). This extract also demonstrated the greatest DPPH scavenging activity (90.13 ± 3.32%) compared to extracts obtained using other solvents [15]. The variation in phytochemical profiles may be due to factors such as climate, soil, season, and the different solvents used for extraction [16].

The benefit of *in silico* models lies in their ability to serve as an initial virtual screening tool to predict the impact of a drug or stimulus on cells or tissues, aiding in the planning of experimental research and clinical trials. However, these models remain theoretical until validated through practical application [17].

During wound healing, the critical phase involves TGF-β recruiting and activating inflammatory cells, such as neutrophils and macrophages, during hemostasis and inflammation. Analysis of mRNA expression in full-thickness wounded samples on day 7 post-injury revealed a significant down-regulation of the inflammatory markers TNF-α and IL-1β in treated wounds compared to untreated wounds [3]. By potentially inhibiting TNF-α and IL-β1, the extract may reduce excessive inflammation, and by interacting with TGF-β1, it may enhance the synthesis of essential components for tissue repair. These findings provide a mechanistic understanding of how the extract can accelerate wound healing.

CONCLUSION

The study shows that phytochemicals present in the methanolic leaf extract of *Plectranthus amboinicus* have a good binding affinity to receptors involved in wound healing. Out of the 28 ligands that were tested, thungberol showed lower binding energy against TNF-α and IL-β1, while (1R,7S,E)-7-Isopropyl-4,10-dimethylenecyclodec-5-enol exhibited lower binding energy against TGF-β1. The results of *in silico* studies suggest that the methanolic leaf extract *of Plectranthus amboinicus* may have the potential to aid in wound healing by interacting with proteins involved in the process. However, additional research involving both *in vitro* and *in vivo* studies are necessary to confirm the effectiveness of these plant compounds in promoting wound healing.

Acknowledgements

The authors would like to acknowledge Kerala Veterinary and Animal Sciences University for providing all necessary support for conducting the studies.

Conflict of interest

The authors declared no conflict of interest.

Financial Support

Financial and technical support provided by the Kerala Veterinary and Animal Sciences University vide order number. KVASU/DAR/A1/2438/2023(1) dt.23/12/2023 is thankfully acknowledged.

ORCID ID

Anoopa Satheesan: https://orcid.org/0009-0007-2335-5890

Siyana Saleem P: https://orcid.org/0009-0007-6847-8843

Suresh N. Nair: https://orcid.org/0000-0002-2178-150X

Bibu John Kariyil: https://orcid.org/0000-0003-0716-6639

Nisha A.R.: https://orcid.org/0000-0001-7121-1954

Deepthi Vijay: https://orcid.org/0000-0001-7384-8123

Prasanna K.S: https://orcid.org/0000-0003-1434-689X

REFERENCES

1. Lodhi S, Vadnere GP. Relevance and perspectives of experimental wound models in wound healing research. Asian J Pharm Clin Res. 2017;10(3):57-62.
2. Tottoli EM, Dorati R, Genta I, Chiesa E, Pisani S, Conti B. Skin wound healing process and new emerging technologies for skin wound care and regeneration. Pharmaceutics. 2020;12(8):735
3. Shady NH, Mostafa NM, Fayez S, Abdel-Rahman IM, Maher SA, Zayed A, Saber EA, Khowdiary MM, Elrehany MA, Alzubaidi MA. Mechanistic wound healing and antioxidant potential of Moringa oleifera seeds extract supported by metabolic profiling, in silico network design, molecular docking, and in vivo studies. Antioxidants. 2022;11(8):1743.
4. Arumugam G, Swamy MK, Sinniah UR. Plectranthus amboinicus (Lour.) Spreng: botanical, phytochemical, pharmacological and nutritional significance. Molecules. 2016;21(3):369.
5. Manjamalai A, Grace VMB. The chemotherapeutic effect of essential oil of Plectranthus amboinicus (Lour) on lung metastasis developed by B16F-10 cell line in C57BL/6 mice. Cancer Invest. 2013;31(1):74-82.
6. Raj A, Nair SN, Abdulvahab R, Ittoop G. In-silico modelling of interaction between environmental xenoestrogens and estrogen receptor of Pacific oyster (Magallana gigas [Thunberg, 1793]) using AutoDock. Informatic studies. 2022:8(1);47-58.
7. Gu Y, Lou C, Tang Y. admetSAR—A valuable tool for assisting safety evaluation. In: QSAR in Safety Evaluation and Risk Assessment. Elsevier; 2024. p. 187-201.
8. Udayan D, Nair SN, Padinchareveetil SK, Thumadath AK. Evaluation of phytochemical constituents, proximate and fluorescence analysis of ethanolic extract and its fractions of Clerodendrum philippinum Schauer found in Wayanad region of Kerala, India. Res J Chem Sci. 2014;4(9):1-6.
9. Mahesh DM, Juliet S, Nair SN, Ravindran R, Shijin MS, Rani SS, Vanishree H. In vitro analysis of 1,8-cineole in the plasma of domestic fowl by Gas Chromatography–Mass Spectrometry. Int J Chem Stud. 2019;7(5):2249-2253.
10. Jumper J, Evans R, Pritzel A, Green T, Figurnov M, Ronneberger O, Tunyasuvunakool K, Bates R, Žídek A, Potapenko A. Highly accurate protein structure prediction with AlphaFold. Nature. 2021;596(7873):583-589.
11. Kausar MA, Ali A, Qiblawi S, Shahid SMA, Izhari MA. Molecular docking based design of Dengue NS5 methyltransferase inhibitors. Bioinformation. 2019;15(6):394.
12. Moon A, Khan D, Gajbhiye P, Jariya M. In silico prediction of toxicity of ligands utilizing admetSAR. Int J Pharma Bio Sci. 2017;8(3):674-677.
13. Cheng F, Li W, Zhou Y, Shen J, Wu Z, Liu G, Lee PW, Tang Y. admetSAR: a comprehensive source and free tool for assessment of chemical ADMET properties. 2012.(http://lmmd.ecust.edu.cn/admetsar2/)
14. Manjamalai A, Narala Y, Haridas A, Grace VMB. Antifungal, anti-inflammatory and GC-MS analysis of methanolic extract of Plectranthus amboinicus leaf. Int J Curr Pharm Res. 2011;2(3):129-136.
15. Swamy MK, Arumugam G, Kaur R, Ghasemzadeh A, Yusoff MM, Sinniah UR. GC-MS based metabolite profiling, antioxidant and antimicrobial properties of different solvent extracts of Malaysian Plectranthus amboinicus leaves. Evid Based Complement Alternat Med. 2017;2017:1517683.
16. Kumar S, Yadav A, Yadav M, Yadav JP. Effect of climate change on phytochemical diversity, total phenolic content and in vitro antioxidant activity of Aloe vera (L.) Burm. f. BMC Res Notes. 2017;10(1):1-12.
17. Ud-Din S, Bayat A. Non-animal models of wound healing in cutaneous repair: In silico, in vitro, ex vivo, and in vivo models of wounds and scars in human skin. Wound Repair Regen. 2017;25(2):164-176.

HOW TO CITE THIS ARTICLE

Satheesan A, Saleem PS, Nair SN, Kariyil BJ, Nisha AR, Vijay D, Prasanna KS. *In silico* assessment of wound healing activity of phytochemicals from methanolic extract of *Plectranthus amboinicus* (Lour.) Spreng. J Phytopharmacol 2024; 13(5):374-382. doi: 10.31254/phyto.2024.13506